Available online at www.sciencedirect.com
ScienceDirect
Journal of Photochemistry and Photobiology A: Chemistry 186 (2007) 202–211
Journal of Photochemistry and Photobiology A:Chemistry
www.elsevier.com/locate/jphotochem

Proton transfer of magnolol in ground and excited states

Hongmei Li, Yunqing Wang, Zhengyu Yan, Huipeng Feng, Yuzhu Hu *

School of Basic Science, China Pharmaceutical University, Nanjing 210038, China

Received 5 June 2006; received in revised form 17 July 2006; accepted 12 August 2006
Available online 23 August 2006

Abstract

Magnolol, 5′,5-di-2-propenyl-[1,1′-biphenyl]-2,2′-diol, has been characterized by steady-state and time-resolved spectroscopy as well as ^{1}H MR and ^{13}C NMR. And the proton transfer reactions both in ground and excited states have been investigated. The binary acid enhances its acidity upon excitation at the first deprotonation reaction and exhibits strong photoacidity. The relationship between the spectroscopic property and the geometric conformation of magnolol with unique biphenyl group has been discussed.

Keywords: Mgnolol; Photoacid; Geomitrc conformation

1. Introduction

Magnolol is the major phenolic element of the plant medicine "Houpo" (*Magnolia officinalis*), which is used in the treatment of chest tightness and asthma. It has various pharmacological functions such as effecting on smooth muscle cells [1,2], inhibiting muscle contraction [3], possessing antioxidant effects approximately thousandfold stronger than alpha-tocopherol [4], increasing cytoplasmic free Ca^{2+} through a phospholipase C-mediated pathway, involving in a new activation mechanism closely associated with intracellular Ca^{2+} mobilization [5], and producing neurotrophic effects in primary cultured rat cortical neurons [6], relieving age-related neuronal loss in the hippocampus [7]. However, less investigation in the spectroscopic property has been reported although the fluorescence and absorption spectra of magnolol has been used in assay of *M. officinalis* and its pharmaceutical preparations.

Proton transfer, both in ground and excited states, plays a key role in many biological processes. The acid-base properties of drug compounds are important to certain biochemical processes such as biological uptake, activity, transport and distribution. As is well known, hydroxyarenes are photoacids of which the acidity greatly increases upon spectroscopic excitation from the ground state. For instance, naphthol, phenol and their substituted derivatives have been extensively investigated both experimentally and theoretically [8–11]. The absorption of a photon by a photoacid triggers a succession of reactions contributing to the overall phenomenon of excited-state proton transfer (ESPT). It has been noticed that the overall action of light on such systems is completely different, though ESPT is an important step in all of them [12–17]. The proton-transfer reactions in ground and excited states of compounds are closely related to their electronic structures. The acidity of hydroxyarene shows a unique dependence on the structure of the photoacid.

We are interested in the photoacidity of magnolol because of its unique structure of biphenyl group (as shown in Fig. 1) and, in particular, because of the relative lack of study on photoacids in the biological literature. Magnolol possesses a symmetrical structure, in which hydroxyl groups are in the *ortho*-position of phenyl group and in the *para*-position of allyl group. The degree of the dihedral between the two benzene rings is affected by the intramolecular H-bonding between the two hydroxyl groups of which deprotonation determines the photoacidity of magnolol. We have noticed the following important features of magnolol related to the investigation of magnolol photochemistry at our experimental conditions:

1. The acidity of neutral magnolol molecule increases dramatically upon electronic excitation. Although magnolol is a binary acid with two hydroxyl groups, only the first proton

* Corresponding author at: Box 41, 24 Tongjia Lane, Nanjing 210009, China. Tel.: +86 25 83271280; fax: +86 25 85391160.
E-mail addresses: Lihongm2001@hotmail.com (H. Li), wyq_cpu@163.com (Y. Wang), yanzhengyujiang@hotmail.com (Z. Yan), fenghuiping6@hotmail.com (H. Feng), njhuyuzu@jlonline.com (Y. Hu).

1010-6030/$ – see front matter © 2006 Elsevier B.V. All rights reserved.
doi:10.1016/j.jphotochem.2006.08.006

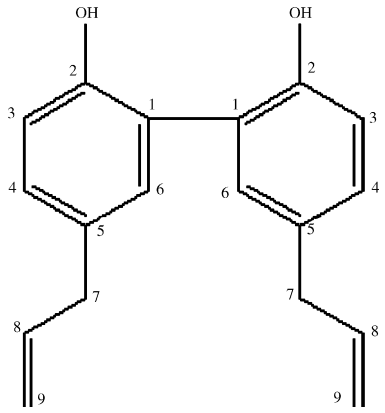

Fig. 1. Structure of magnolol.

dissociation of excited-state has been observed. In aqueous solutions the pK_{a1} value decreases by about 7 units upon excitation.

2. Neutral magnolol can transfer its proton to water but not to methanol in the excited state, demonstrating single-peak fluorescence (around 400 nm) in aqueous solution. The emission band of excited monoanic magnolol HA^{-*} appears in a wide pH range from 0 to 14 with the intensity dependent on pH. The emission band of excited neutral form H_2A^* at around 355 nm appears in acidic and neutral methanol and almost disappears in water even at sufficiently low pH because of the strong photoacidity and the occurrence of proton-quenching. An apparent pK^*_{a1} of excited-state is 0.57 from determination by fluorescence titration.
3. The first proton dissociation of ground-state results in red-shifted absorption. The pK_{a1} 7.54 and pK_{a2} 14.38 of ground-state have been obtained by fluorescence titration. Steady-state and time-resolved spectroscopy and ^{1}H NMR and ^{13}C NMR indicate no other reaction but the second deprotonation occurs in strongly basic aqueous solution. Along with the second deprontonation, an unusual blue-shifted absorption has been observed and attributed to the change in geometric conformation of biphenyl group which takes place in the transition from monoanion HA^- to dianion A^{2-} of ground-state.

2. Experiment

Magnolol was isolated from the cortex of *M. officinalis* Rhed. The 99% purity was determined by HPLC. Water was deionized and redistilled. Solvents were used without detectable fluorescent impurities. The buffer solutions with pH from 4 to 12 were prepared with 0.1 mol L^{-1} solution of sodium phosphate and 0.1 mol L^{-1} solution of hydrochloric acid, those with pH < 4 were prepared with hydrochloric solution and those with pH > 12 with sodium hydroxide solution respectively. The pH was measured with a PHS-2C pH-meter (Shanghai Analytical Instrumental Factory, China). The ionic strength of the buffers was adjusted to 0.1 mol L^{-1} with sodium chloride.

All experiments were performed at room temperature (22 °C). The UV absorption spectra were recorded on a Shimadzu UV-2101PC spectrometer. Steady-state fluorescence spectra of nondeoxygenated solutions were recorded on a Shimadzu FR-5301 spectrofluorometer. Transient fluorescence was detected using the time-correlated single-photon counting (TCSPC) method on an Edinburgh instrument. ^{1}H NMR and ^{13}C NMR spectra were recorded on Varian Gemimi series 300 MHz spectrometer.

3. Result

3.1. Absorption spectra and absorption spectroscopic titration

During the study of the pH dependence of absorption and emission, aggregation of magnolol should be avoided. Magnolol shows good linearity in the Beer's law plot ($\varepsilon = 6650$ mol L^{-1} cm^{-1} at 284 nm) up to 0.1 mmol L^{-1} in neutral aqueous solution. Thus, the absorption spectroscopic titration was performed in water with the concentration of 3×10^{-5} mol L^{-1}.

We investigated the absorption and fluorescence spectra in aqueous solutions with pH from −0.3 to 14.7. In order to discuss the results distinctly, the spectral data were divided into three parts: (1) the strongly acidic region, pH from −0.3 to 3; (2) the weakly acidic–basic region, pH from 6 to 10; (3) the strongly basic region, pH from 13 to 14.7.

The absorption spectra at all pH values were shown in Fig. 2A, C and E, demonstrating transformation between neutral, monoanionic and dianionic species. At low pH, the low-energy absorption peak with a maximum at 284 nm appeared in aqueous solution. With pH increasing from 6 to 9, the low-energy absorption gradually shifted to a new peak with a maximum at 316 nm. Two clear isoabsorptive points at 267 and 294 nm were observed. The spectral transformation could be attributed to the first deprotonation reaction, the absorption band at 284 nm and that at 316 nm were assigned to the neutral magnolol H_2A and the monoanionic magnolol HA^-, respectively. With further basification up to pH 13, both the absorption maximum did not change. Upon increasing concentration of NaOH from 0.1 to 6.0 mol L^{-1}, the absorption peak with a maximum at 316 nm was gradually blue-shifted to 309 nm. The first deprotonation constant of ground-state pK_{a1} could be determined by monitoring the absorbance at 316 nm where H_2A has no absorbance. The UV-absorbance titration curve at 316 nm was presented in Fig. 3A with the inflection point at around pH 7.37.

3.2. Steady-state fluorescence spectra in methanol solution

The emission of magnolol in methanol was different from that in water. The emission bands in neutral methanol coincided with that in acidic methanol with a maximum at 355 nm. With addition of NaOH to methanol, the emission band at 355 nm disappeared and a new emission band at 400 nm emerged, see Fig. 4. In methanol with addition of $HClO_4$ up to 0.1–3.6 mol L^{-1}, a strong proton quenching was observed. The quenching curve was shown in Fig. 5. Water acted effectively to change the

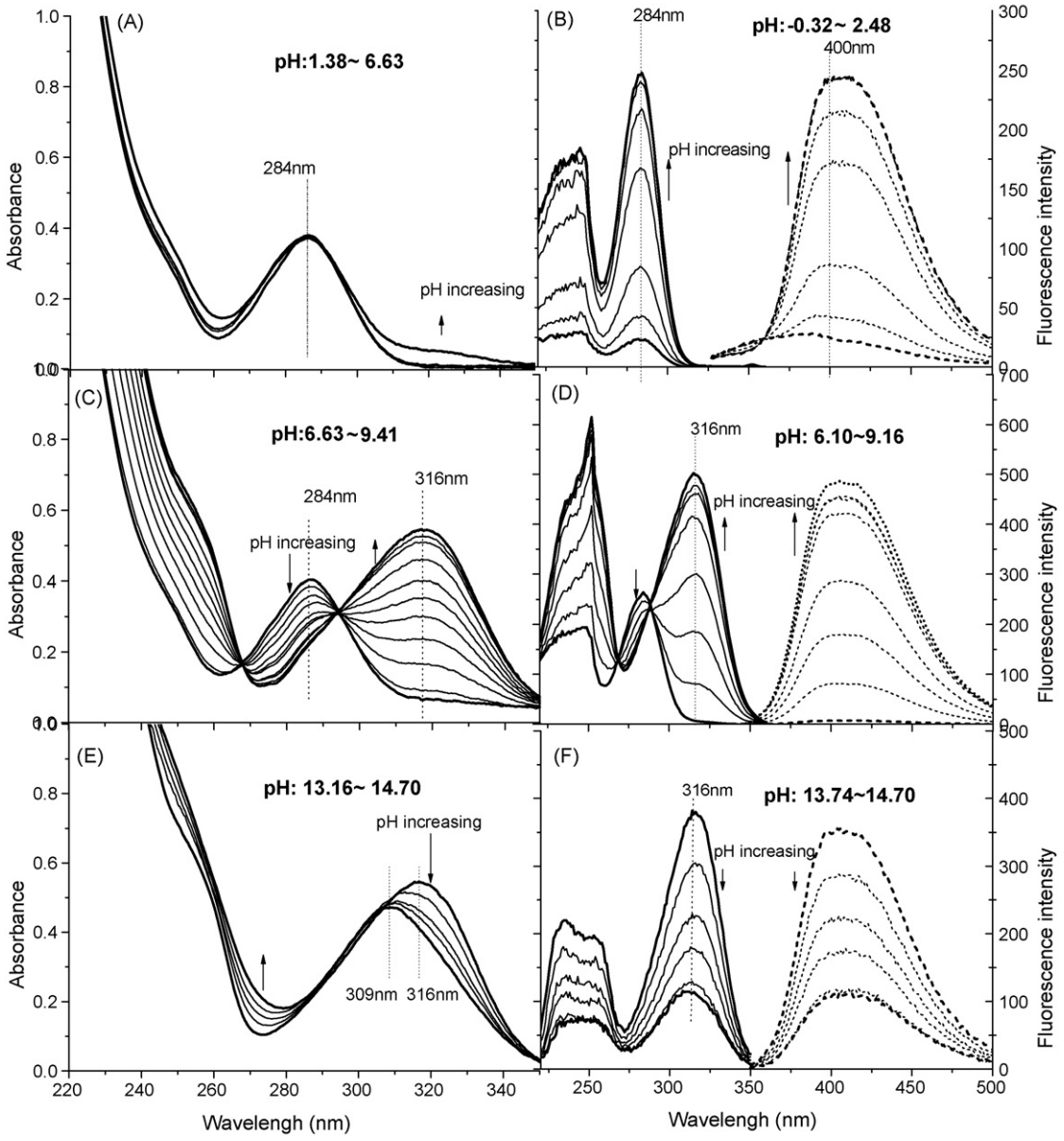

Fig. 2. Absorption spectra and fluorescence spectra of magnolol in water as function of pH: (A) absorption spectra in acidic pH region; (B) fluorescence spectra in acidic region; (C) absorption spectra in weak acidic–basic region; (D) fluorescence spectra in weak acidic–basic region; (E) absorption spectra in strong basic region; (F) fluorescence spectra in strong basic region. In (B), (D) and (F) the excitation spectra were expressed as the solid lines and the emission spectra expressed as the dash lines. The excitation wavelengths were shown on the excitation spectra.

emission spectra of magnolol in methanol. With increasing concentration of water, the emission around 355 nm decreased in intensity and the new emission around 400 nm appeared with increasing intensity, as shown in Fig. 6. Meanwhile, we noticed that excitation spectra were also dependent on water concentration. The low-energy excitation underwent a blue-shift from 292 nm in pure methanol to 284 nm in pure water which agree with the absorption spectra in methanol and in water. Thus, we assigned the emission band at 355 nm to H_2A^* and that at 400 nm to HA^{-*}. According to the emission spectra in aqueous solution under various pHs and in the mixtures of water–methanol, it was concluded that magnolol displayed effective ESPT to water, but no ESPT to methanol.

3.3. Steady-state fluorescence spectra and fluorescence titration in aqueous solution

In aqueous solution with pH from 0 to 14, the emission band remained around 400 nm with pH dependence of intensity. The excitation spectra at pH 6–9 matched the absorption spectra well, see Fig. 2C and D. With pH increasing, the excitation peak shifted from 284 to 316 nm, demonstrating that the excited species changed from neutral magnolol into monoanionic form based on the ground-state deprotonation reaction. Thus, the pK_{a1} of ground-state also could be determined by monitoring the emission upon excitation at 316 nm. The fluorescence titration curve is presented in Fig. 3C. The inflection

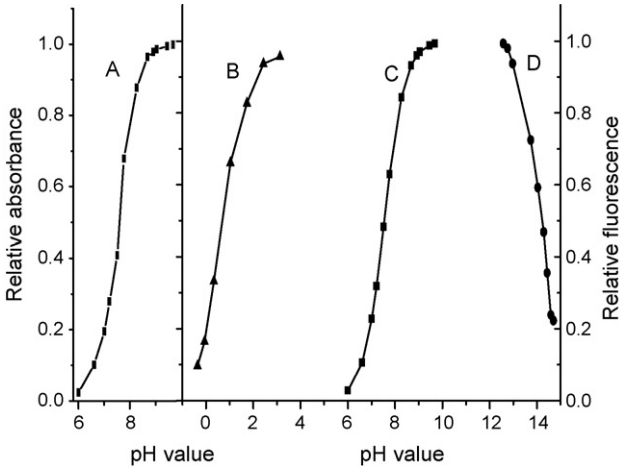

Fig. 3. Steady-state titration curves of magnolol in aqueous solution. (A) The absorbance data at 316 nm at pH 6–10; (B) the fluorescence data with the excitation at 284 nm at pH −0.5–4; (C and D) the fluorescence data with the excitation at 316 nm at pH 6–10 and 12–14.8.

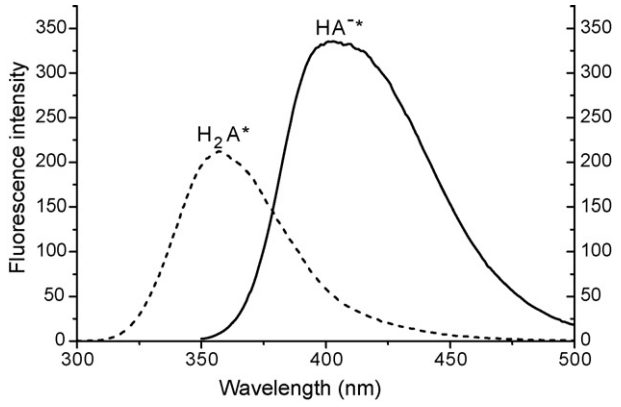

Fig. 4. Emission spectra of magnolol in methanol with 0.1 mol L^{-1} $HClO_4$ (the dash line) and with 0.1 mol L^{-1} NaOH (the solid line).

point at the titration curve was observed around pH 7.54. Similar to the absorption spectra, the emission is not influenced by the pH change from 10 to 12. In strongly basic region, an increase in concentration of NaOH from 0.1 to 6.0 mol L^{-1} resulted in a

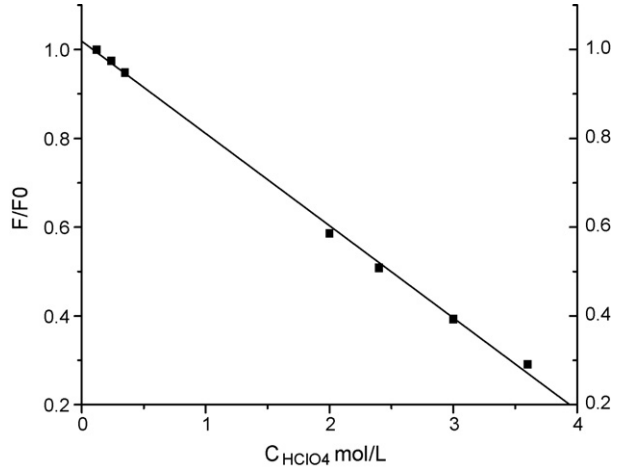

Fig. 5. Quenching of magnolol by $HClO_4$ in methanol.

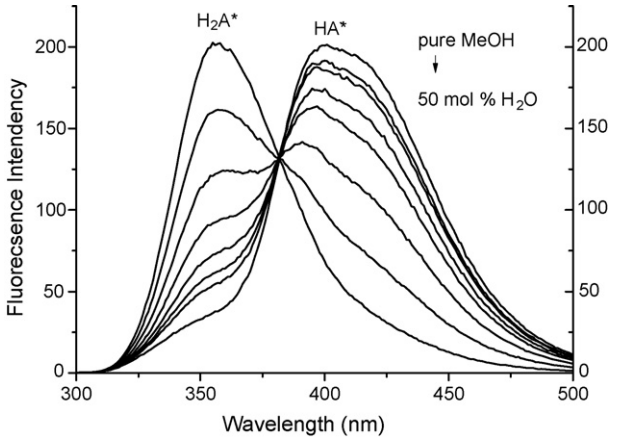

Fig. 6. Emission spectra of magnolol in methanol-water mixtures. Water molar fractions (from top to bottom for H_2A^* band at 355 nm) are: 0, 0.101, 0.183, 0.252, 0.309, 0.359, 0.402 and 0.528).

quick decrease in emission intensity. The new spectral transition may be due to the following possible reactions: (1) the second proton dissociation of ground-state, (2) the second proton dissociation of excited-state, and (3) production of other compounds. Unlike the blue-shifted absorption spectra under the same condition, the excitation peak remained at 316 nm, which indicated the excited band was due to the ground-state monoanion HA^- and the emission came from the excited monoanion HA^{-*}. In addition, the ^1H NMR and ^{13}C NMR spectra and the time-resolved measurement at various pH values showed no production of other compounds (to be discussed in the latter section). Thus, we attributed the spectral transformation to the second proton dissociation of ground-state. The dissociation constant pK_{a2} was determined by fluorescence titration at pH 12.2–14.8. The titration curve was presented in Fig. 3D with the inflection point at pH 14.38. In the strongly acidic region another spectra transition occurred. With decreasing pH from 6 to 4.0, the emission did not change significantly. Nevertheless, from pH 4.0 to 0.3, the intensity decreased without change in the emission peak. With further acidification of HCl more than 1.0 mol L^{-1}, the emission band underwent a significant blue-shift with a decrease in intensity, see Fig. 2B. This indicated the higher concentration of proton had restrained the occurrence of ESPT of neutral magnolol, and as a result the emission at 400 nm from HA^{-*} decreased. Because of the proton quenching, the emission from the species H_2A^* was weak. The apparent pK^*_{a1} was determined without taking into account proton quenching on excited monoanion HA^{-*}. The titration curve was shown in Fig. 3B.

3.4. Time-resolved measurement and NMR spectra

Magnolol showed ESPT in water so effective that only the emission band of excited monoanionic HA^{-*} was observed when pH > 0, which was especially obvious in the time-resolved measurement. The time-resolved signals in aqueous solutions at pH = 4.0, 7.0, 9.0, 12.0 and 14.0 were detected at 400 nm using TCSPC technique. All the fluorescence decays were single-exponential and the deconvolution fits indicated a constant lifetime of 4.5 ns with the $\chi^2 = 1.06$–1.12. Fig. 7 is an

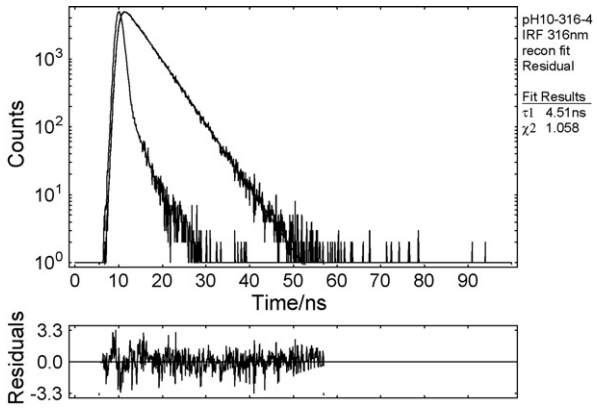

Fig. 7. Time-resolved fluorescence emission of magnolol in aqueous solution at pH 10.

example of the experimental kinetic data fitting. The dot curve is the time-resolved emission data and the solid curve is the theoretical calculation for the component convoluted with the instrument response function (IRF). It is confirmed that only one emission form exists in aqueous solutions in such wide pH range.

To confirm only the second deprotonation reaction of ground-state occurred in the strongly basic region, we measured the ^{1}H NMR and ^{13}C NMR spectra in 0.1 and 6 mol L^{-1} NaOH solutions, respectively. The experiments were performed in 4/6 (v/v) CD_3OD–D_2O mixture because of the poor solubility of magnolol in pure water. The H^1 NMR and C^{13} NMR spectra were presented in Figs. 8 and 9, respectively. Table 1 shows the comparison of the chemical shifts under different pH condition. No distinct change in the signals of all hydrogen atoms was observed, which demonstrated that no other transition but the proton dissociation of monoanionic magnolol HA^- occurred. The number of the dissociated protons was not directly detected because of the fast exchange of active hydrogen atoms. The average chemical shifts of all the atoms at the corresponding positions in the benzene rings were caused by the symmetrical biphenyl structure. However, the dissociation reactions can be characterized by the chemical shift of the carbon atom (C2) bonding directly to the hydroxyl group. The signals of

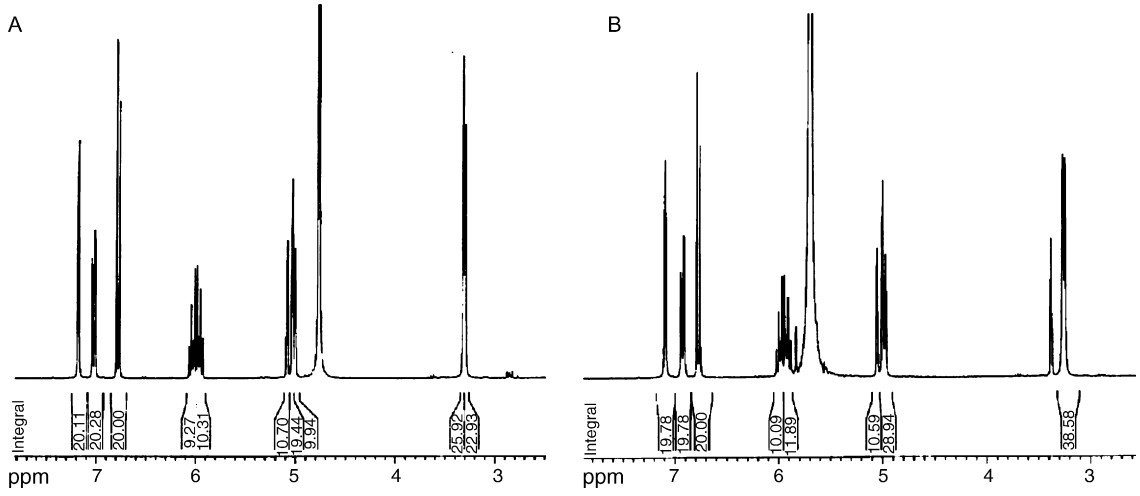

Fig. 8. ^{1}H NMR spectra of magnolol in 4/6 (v/v) CD_3OD–D_2O mixture with NaOH 0.1 and 6 mol L^{-1}.

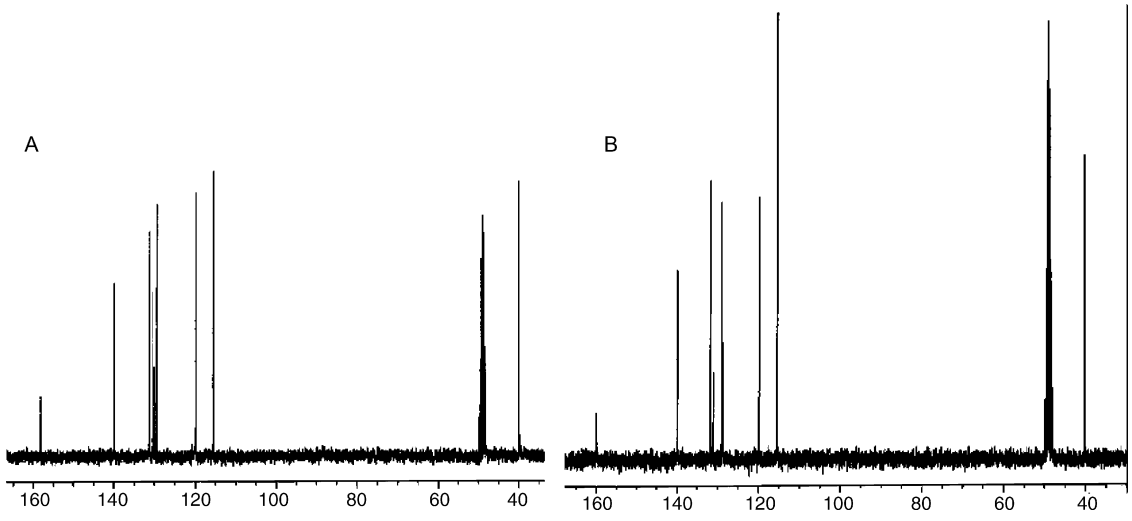

Fig. 9. ^{13}C NMR spectra of magnolol in 4/6 (v/v) CD_3OD–D_2O mixture with NaOH 0.1 and 6 mol L^{-1}.

Table 1
Comparison of the chemical shifts of magnolol under different pH condition

Atom	In $CDCl_3$[a]	In MW[b] with 0.1 M NaOH	In MW[b] with 6 M NaOH
C1	123.9	130.00	128.58
C2	150.9	158.14	160.11
C3(H3)	116.6	119.90 (6.774)	119.80 (6.701)
C4(H4)	129.9	129.37 (7.031)	128.98 (6.868)
C5	133.2	130.42	131.02
C6(H6)	131.2	131.19 (7.175)	131.71 (7.025)
C7(H7)	39.3	40.00 (3.300)	40.20 (3.189)
C8(H8)	137.5	139.87 (5.990)	139.95 (5.877)
C9(H9)	115.8	115.58 (5.032)	115.42 (4.932)

[a] From Ref. [19].
[b] Represented the (v/v) 4/6 CD_3OD–D_2O mixture.

C2 atom shifted to the lower field with the deprotonation of hydroxyl group. The magnolol exhibited its neutral form with 150.9 ppm of C2 and 123.9 ppm of C1 in $CDCl_3$ (adapted from Ref. [18]) and the monoanionic form with 158.1 ppm of C2 and 130.00 ppm of C1 in 0.1 mol L^{-1} NaOH CD_3OD–D_2O solution and the mixture of monoanionic and dianionic forms with 160.11 ppm of C2 and 128.38 ppm of C1 in 6 mol L^{-1} NaOH CD_3OD–D_2O solution, respectively.

4. Discussion

4.1. Proton dissociation in ground-state and excited-state in aqueous solution

From the discussion above, the relationship between the spectroscopy and the proton transfer reactions of magnolol was shown in Scheme 1.

Depending on pH, three ground-state species exists in the neutral form H_2A, the monoanionic form HA^- and the dianionic form A^{2-}. We associate the 284 nm absorption at lower and neutral pH with H_2A, the 316 nm absorption at high pH with HA^- and the 309 nm absorption at higher pH with A^{2-}. The equilibrium between H_2A and HA^-, characterized by absorption titration with a pK_{a1} 7.34, is about 2.5 units lower than that of phenol which has been reported with the ground-state pK_a 9.82 and the excited-state pK_a^* 4 [19,20]. It demonstrates a clear electron-withdrawing action of benzene ring. The substituted phenol with cyanide, the strong electron-withdrawing group,

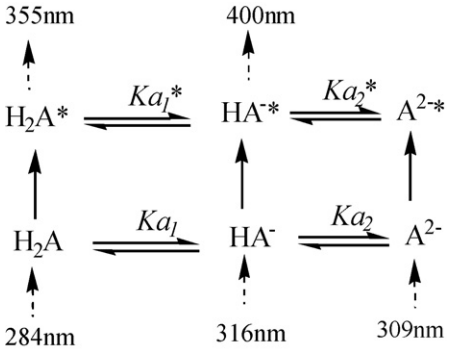

Scheme 1. Relation between the spectroscopy and proton transfer reactions of magnolol.

was also reported with low pK_a value, e.g., *o*-cyanophenol with pK_a 6.97 and pK_a^* 0.66 [21]. The pK_{a1} and pK_{a1}^* (apparently 0.57) of magnolol is similar to those of *o*-cyanophenol. Obviously, the Hückel coefficient of substituted group of phenyl at the *ortho*-position is large, and close to that of cyanide.

It is the acid–base equilibriums in ground state that results in the pH dependence of fluorescence intensity at pH > 4. The first deprotonation of ground-state causes an increase in fluorescence intensity upon excitation at 316 nm at pH 6–9. The second deprotonation in ground-state causes a decrease in fluorescence intensity upon excitation at 316 nm at pH > 12. The pK_{a1} is 7.56 determined by fluorescence titration, quite closed to that by absorption titration. The pK_{a2} value is 14.38 from determination by fluorescence titration. In the range pH < 4, the decrease in fluorescence intensity is caused by the first excited deprotonation reaction and proton quenching. The apparent pK_{a1}^* is 0.57 determined by fluorescence titration. The value should be lower than that by kinetics method due to the effect of proton quenching. Another approach for pK_a^* determination is the Förster equation [22]:

$$pK_a - pK_a^* = \frac{N_A h(\nu_{abs} - \nu'_{abs})}{2.303RT}$$

where ν_{abs} and ν'_{abs} are the frequencies of the lowest absorption bands of the neutral form and the deprotonic form, N_A the Avogadro number and h is the Planck constant. However, in practice the validity of Förster approach is questionable due to solvent relaxation around the conjugated acid–base pair [10,23]. In this case, the pK_a^* value by Förster approach of 3.6 is 3 units larger than that by fluorescence titration. The summary of all the pK_a values obtained by different methods is presented in Table 2.

According to the pK_a determined by fluorescence titration, the pH dependence of the molar fraction, α, of every species of

Table 2
pK_a values of magnolol in the ground and excited states

Method	pK_{a1}	pK_{a2}	pK_{a1}^*
UV-absorbance titration	7.37		
Fluorescence titration	7.54	14.38	0.57
Föster equation			3.60

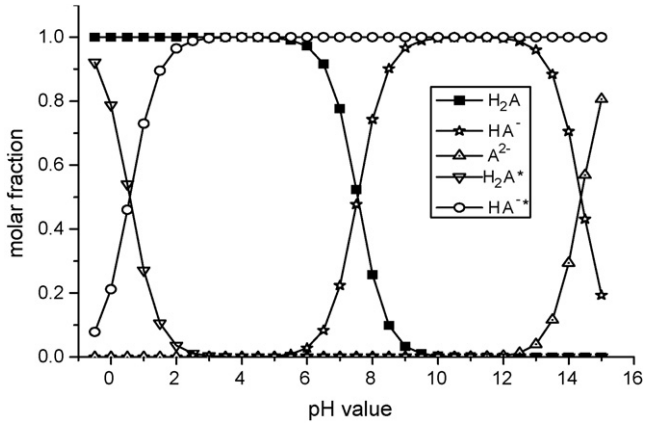

Fig. 10. The molar fraction distribution of the round and excited forms of magnolol in ependence upon pH (calculated from the determined pK_{a1}, pK_{a2} and pK^*_{a1}).

magnolol in the ground and excited states is shown in Fig. 10. H_2A is the dominating ground-state form at pH < 6. HA^- is the dominating ground-state forms at pH 9–12. HA^- gradually becomes A^{2-} at pH > 12. With respect to the excited forms, HA^{-*} is overwhelming at pH > 4. H_2A^* exists in a strongly acidic region, but its emission is rather weak in aqueous solution because proton quenching becomes strong in such pH condition. With the assumption that the ground-state form has the same excitation-efficiency and the excited form has the same emission-efficiency under various pH conditions, the relative concentration of HA^{-*} can be evaluated. We define $X_{HA^{-*},284} = \alpha_{H_2A} \cdot \alpha_{HA^{-*}}$ when H_2A is excited, and $X_{HA^{-*},316} = \alpha_{HA^-} \cdot \alpha_{HA^{-*}}$ when HA^- is excited. The curves of $X_{HA^{-*}}$ is shown in Fig. 11. The curve of I_{316} is in excellent agreement with the curve of $X_{HA^{-*},316}$ in rather wide pH range, which confirms that the pH dependence of fluorescence intensity is caused by the acid–base equilibriums of the ground state at pH > 4. By comparison between the curves of I_{284} and $X_{HA^{-*},284}$, it is found that the two lines are identical at lower pH but discrepant at higher pH, which is resulted from proton quenching on HA^{-*} at low pH. So the pK^*_{a1} value measured by fluorescence titration should be lower than the actual value.

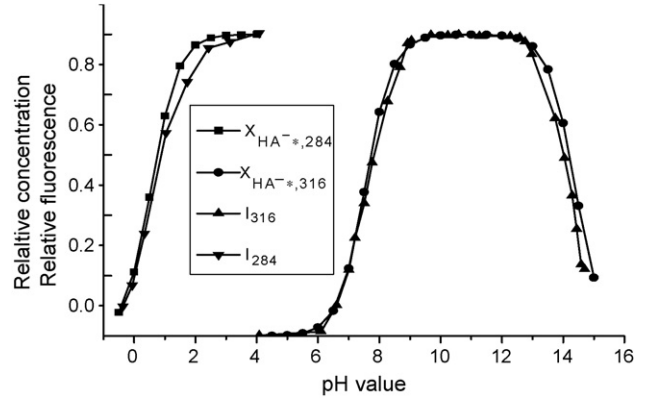

Fig. 11. Comparison of the emission intensity with the relative concentration of HA^{-*} ($X_{HA^{-*}}$) under various pH conditions.

4.2. Water concentration dependence of ESPT in water–methanol mixtures

Magnolol shows no ESPT in pure methanol. But the EPST is highly sensitive to the presence of water and very little amount of water induces a small but detectable 400 nm-emission from HA^{-*} in methanol, see Fig. 6. With the further addition of water, the increase in the HA^{-*} emission and the decrease in the H_2A^* emission indicates strengthened ESPT. We have noticed the emission spectra showed a strong variation in the methanol-rich region and moderate change in the water-rich region, at higher water concentrations the emission band is the same as that in pure water, but the intensity decreased with water concentration increasing. Similar effect also has been observed for other photoacids, e.g., cyano-naphthol and hydroyquinoline [24–27]. It is attributed to (a) preferential solvation of the hydroxyl moiety by water and (b) gradual change in the solvation energy of the intramolecular charge transfer. The recent kinetics analysis has demonstrated that the dissociation rate constant was proportional to a power of water concentration for various photoacids, which affected the spectral behaviors of photoacids in methanol-water mixture [9,25,26].

4.3. Proton quenching in methanol

As demonstrated in previous section, in neutral and acidic methanol, the excited species is neutral magnolol H_2A^*. Unlike that in water, the emission from H_2A^* shows large fluorescence efficiency in neutral methanol and in 0.1 mol L^{-1} $HClO_4$, see Figs. 4 and 6. Upon further addition of $HClO_4$, the intensity decreases with a linear dependence upon the concentration of $HClO_4$.

The quenching does not fit the Stern–Volmer equation in which F_0/F is expected to be linearly dependent upon the concentration of quencher with a slope equal to K_D ($K_D = k_q\tau_0$), the Stern–Volmer quenching constant. In contrast, as shown in Fig. 5, F/F_0 is linearly dependent upon the concentration of the quencher $HClO_4$, shown as Eq. (1) with $R^2 = 0.999$:

$$\frac{F}{F_0} = 1.02 + 0.21 c_{HClO_4} \tag{1}$$

Eq. (1) is reasonable:

$$\frac{F}{F_0} = \frac{F_0 - (F_0 - F)}{F_0} = 1 - \frac{F_q}{F_0} \tag{2}$$

where F_0 and F are the fluorescence intensity in the absence and presence of quencher, respectively, and F_q is the fluorescence intensity quenched by quencher. The fluorescence intensity observed for a fluorophore is proportional to its concentration in the excited state. Thus F_q/F_0 is equal to $[H_2A^*]_q/[H_2A^*]_0$, where $[H_2A^*]_q$ and $[H_2A^*]_0$ are the populations of the excited-state fluorophore quenched by $HClO_4$ and decayed by fluorescence in the absence of quencher, respectively:

$$[H_2A^*]_q = \int k_q c_{HClO_4} C_{H_2A^*}\, dt \tag{3}$$

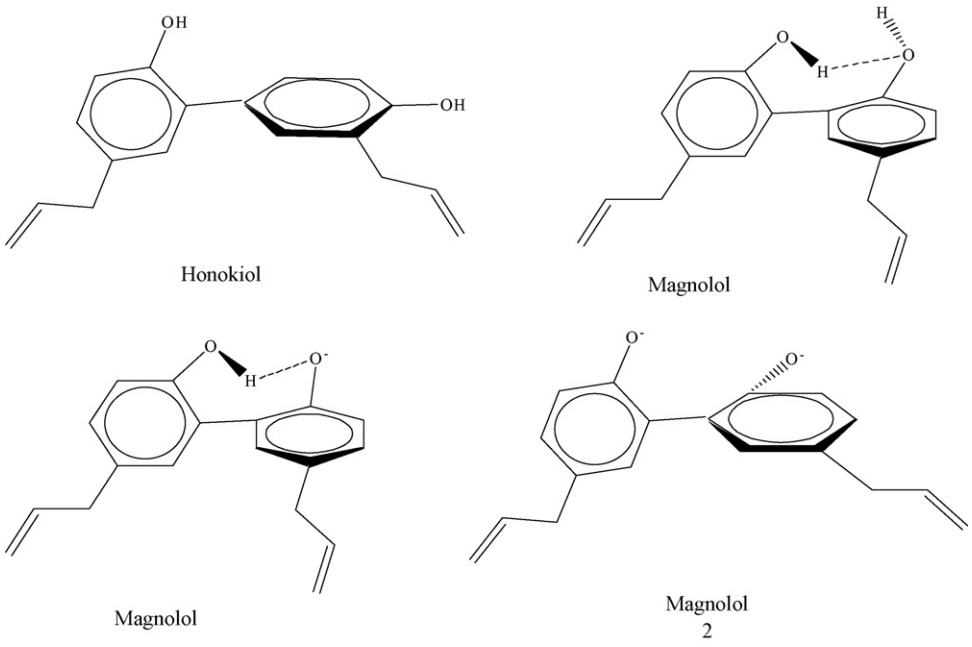

Fig. 12. Geometric structures of Honokiol and neutral, monoanionic and dianionic Magnolol.

$$[H_2A^*]_0 = \int k_0 c_{H_2A^*}\, dt \quad (4)$$

Then

$$[H_2A^*]_q = k_q c_{HClO_4} \int c_{H_2A^*}\, dt \quad (5)$$

$$[H_2A^*]_0 = k_0 \int c_{H_2A^*}\, dt \quad (6)$$

where k_q and k_0 are the quenching rate constants and the fluorescence rate in the absence of quencher, respectively. Thus, the quenching equation is established as follows:

$$\frac{F}{F_0} = 1 - \frac{k_q}{k_0} c_{HClO_4} \quad (7)$$

We can conclude that the physical signification of the slope is k_q/k_0 in Eq. (1).

4.4. Relationship between the spectra and the geometric structures

With the proton dissociation from hydroxyl group, to our knowledge, the absorption spectra of aromatic alcohols undergo a red-shift, often concomitant with a hyperchromic effect because the conjugated system becomes larger with the participation of the orbital of the deprotoned oxygen atom. In comparison with neutral magnolol H_2A, the low-energy absorption band of the monoanion HA^- underwent a red-shift from 284 to 316 nm, with an increase in mole absorbance from 6450 mol L^{-1} cm^{-1} (determined at pH 4) to 8910 mol L^{-1} cm^{-1} (determined at pH 11). However, the low-energy absorption band of the dianion A^{2-} underwent a significant blue-shift concomitant with a hypochromic effect in contrast with the behavior of monoanion HA^-, see Fig. 2C and E.

The geometric conformation of biphenyl in magnolol should be considered to explain the unusual absorption blue-shift. Among substituted biphenyl compounds, the dihedral angle between two benzene rings varies from 0° (co-planar) to 90°. The variations of the angle are not only due to the quantity, the property and the size of the substituted groups, but also the substituted position [28–30]. The crystal X-ray diffraction of magnolol has demonstrates a dihedral angle of 44.9°, even substituted by the fairly large allyl [31]. This smaller angle induces the best possible intramolecular H-bonding between the two rings: O···O distance is 2.60 Å. Honokiol, 5′,5-di-2-propenyl-[1,1′-biphenyl]-2,4′-diol (as shown in Fig. 12) is one isomer of magnolol. Nevertheless, because of the positions of the hydroxyl groups, its crystal X-ray diffraction demonstrates an angle of 57.14° [32], rather larger than that of magnolol due to the absence of the intramolecular H-bonding between benzene rings. Therefore, the intramolecular H-bonding plays an important role in the geometric conformation of magnolol.

When neutral magnolol H_2A dissociates one proton from one of the hydroxyl groups, the intramolecular H-bonding is strengthened. The smaller the dihedral angle is, the stronger the two benzene rings are conjugated. With regard to the dianion of magnolol A^{2-}, the dissociation of both the two protons leads to the vanishing of the intramolecular H-bonding, which enlarges the dihedral. In addition, the strong coulombic repulsion by the negative charges on the two rings strengthens the twisting further. The enlarged dihedral angle weakens the conjugation of the two benzene rings system. Accordingly, an absorption blue-shift and hypochromic effect takes place. The proposed conformation of monoanionic and dianionic magnolol is presented with that of neutral magnolol and honokiol in Fig. 12.

The photoacidity is, in the traditional view, supposed to arise from an intramolecular charge transfer (ICT) from the oxygen atom to the aromatic ring system [8]. However, recently theoreti-

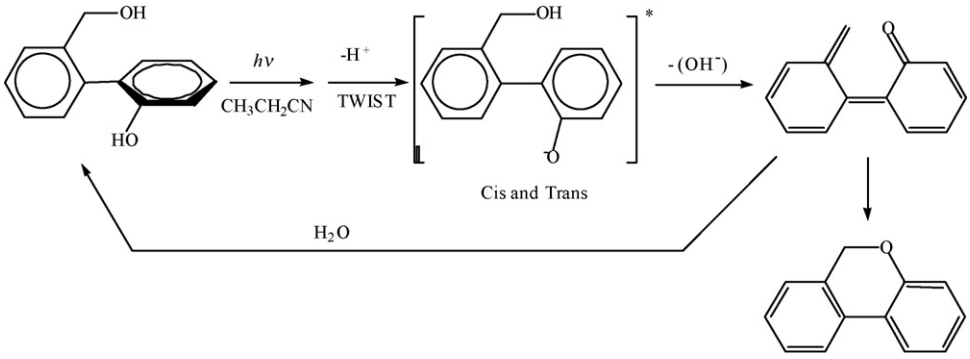

Fig. 13. Proposed mechanism for photocyclization of 2-(2′-hydroxyphenyl)benzyl alcohol. Adapted from Ref. [34].

cal calculations on phenol and cyanophenol, as well as naphthol and cyanonaphthol, show that the ICT is larger in the deprotonic form than in the acid form upon excitation [8,11]. The excited-state reaction thus becomes more downhill, resulting in enhanced photoacidity. Noam Agam [9] has interpreted why excited-state ICT from oxygen center is larger in the deprotonic form than that in the acid form by adopting the notions of aromaticity. All the factors strengthening aromaticity in the excited-state anion facilitate to stabilize the excited anion. As for magnolol, the geometry of biphenyl is probably the important reason for the photoacidity. Huang et al. have reported a photocyclization of 2-(2′-hydroxypheny)benzyl alcohol in aqueous solution and proposed the mechanism involving a very fast twisting in the biphenyl to a more planar geometry which is probably associated with deprotonation of the phenol moiety of excited-state [33,34], see Fig. 13. We consider that the monoanion of magnolol turns more planar during the transition from the ground-state to the excited-state, and then a new conjugated system is established, generating a $4n + 2$ ($n = 3$) aromatic system by delocalizing a pair of oxygen electrons to the phenyl rings, as a result, the excited monoanion HA^{-*} is stabilized and magnolol exhibits a strong photoacidity. As for the excited-state dianion A^{2-*}, the larger dihedral angle weakens the conjugated system between the two benzene rings and destabilized the excited dianion A^{2-*}, which probably accounts for no emission of A^{2-*} was observed.

5. Conclusion

Magnolol, the natural drug compound is classified as photoacid. Its acidity shows a unique dependence on the structure of the photoacid. With the properties of strong ESPT reactivity and the two acid–base equilibriums and the bright fluorescence, magnolol can be a candidate of fluorescence probe, especially a pH probe with wide range pH. By summarizing the absorption and fluorescence and NMR spectra in various pH values, we assume that the geometric conformation of magnolol plays an important role in its spectral properties.

Acknowledgement

This research was supported by Youth Foundation of China Pharmaceutical University (D0318).

References

[1] J.H. Chen, C.C. Wu, G. Hsiao, M.H. Yen, Naunyn. Schmiedebergs Arch. Pharmacol. 368 (2) (2003) 127–133.
[2] C.H. Ko, H.H. Chen, Y.R. Lin, M.H. Chan, Planta Med. 69 (6) (2003) 532–536.
[3] H. Zhai, K. Nakade, Y. Mitsumoto, Y. Fukuyama, Eur. J. Pharmacol. 474 (2–3) (2003) 199–204.
[4] Y.C. Lu, H.H. Chen, C.H. Ko, Y.R. Lin, M.H. Chan, Naunyn. Schmiedebergs Arch. Pharmacol. 368 (4) (2003) 262–269.
[5] Y.R. Lin, H.H. Chen, C.H. Ko, M.H. Chan, Neuropharmacology 49 (4) (2005) 542–550.
[6] N. Matsui, H. Nakashima, Y. Ushio, T. Tada, A. Shirono, Y. Fukuyama, K. Nakade, H. Zhai, Y. Yasui, N. Fukuishi, R. Akagi, M. Akagi, Biol. Pharm. Bull. 28 (9) (2005) 1762–1765.
[7] C.-H. Wu, C.-W. Chen, H.-C. Chen, W.-C. Chang, M.-J. Shu, J.-S. Hung, J. Pharmacol. Sci. 99 (4) (2005) 392–399.
[8] G. Granucci, J.T. Hynes, P. Millié, T.-H. Tran-Thi, J. Am. Chem. Soc. 122 (2000) 12243–12253.
[9] N. Agmon, J. Phys. Chem. A 109 (2005) 13–35.
[10] L.G. Arnaut, S.J. Formosinho, J. Photochem. Photobiol. A: Chem. 75 (1993) 1–20.
[11] N. Agmon, W. Retting, C. Groth, J. Am. Chem. Soc. 124 (2002) 1089.
[12] M. Zimmer, Chem. Rev. 102 (2002) 759–781.
[13] N.P. Malikova, G.A. Stepanyuk, L.A. Frank, S.V. Markova, E.S. Vysotski, J. Lee, FEBS Lett. 554 (2003) 184–188.
[14] J.K. Lanyi, Annu. Rev. Physiol. 66 (2004) 665–688.
[15] M.L. Paddock, G. Feher, M.Y. Okamura, FEBS Lett. 555 (2003) 45–50.
[16] V. Shafirovich, N.E. Geacintov, Top. Curr. Chem. 237 (2004) 129–157.
[17] K. Das, K.D. Ashby, J. Wen, J.W. Petrich, J. Phys. Chem. B 103 (1999) 1581–1585.
[18] X. Wang, Y.Q. Wang, Y.L. Geng, F.W. Li, J. Chromatogr. A 1036 (2004) 171–175.
[19] E.L. Wehry, L.B. Rogers, J. Am. Chem. Soc. 87 (1965) 4234.
[20] N. Mikami, Bull. Chem. Soc. Jpn. 68 (1995) 683.
[21] S.G. Schulman, W.R. Vincent, W.J.M. Underberg, J. Phys. Chem. 85 (1981) 4068.
[22] Z. Grabowski, W. Rubaszewska, J. Chem. Soc. Faraday Trans. 1 (73) (1977) 11.
[23] W.H. Mulder, J. Photochem. Photobiol. A: Chem. 161 (2003) 21–25.
[24] K.M. Solntsev, C.E. Clower, L.M. Tolbert, D. Huppert, J. Am. Chem. Soc. 127 (2005) 8534–8544.
[25] K.M. Solntsev, E.N. Sullivan, L.M. Tolbert, S. Ashkenazi, P. Leiderman, D. Huppert, J. Am. Chem. Soc. 126 (2004) 12701–12708.
[26] K.M. Solntsev, D. Huppert, N. Agmon, L.M. Tolbert, J. Phys Chem. A 104 (2000) 4658–4669.
[27] E. Pines, D. Pines, T. Barak, B.Z. Magnes, L.M. Tolbert, J.E. Haubrich, Ber. Bunsen. Phys. Chem. 102 (1998) 511–517.

[28] K. Nakatsu, H. Yoshioka, K. Kinoshita, Tetrahedron Lett. 23 (1982) 1173–1176.
[29] P. Singh, J.D. Mckinney, Acta Cryst. B35 (1979) 259–262.
[30] M.J. Hamor, T.A. Harmor, Acta Cryst. B34 (1978) 2994–2997.
[31] Y. Wang, M.C. Cheng, J.S. Lee, F.C. Chen, J. Chin. Chem. Soc. 30 (1983) 215–221.
[32] M.J. Fullmer, R.C. Haltiwanger, N. Troupe, D.S. Eggleston, Acta Cryst. C50 (1994) 1966–1967.
[33] C.G. Huang, K.A. Beveridge, P. Wan, J. Am. Chem. Soc. 113 (1991) 7676.
[34] P. Wan, D. Shukla, Chem. Rev. 93 (1993) 571–584.